From Membranes to Membrane Machines

Reinhard Lipowsky

MPI für Kolloid– and Grenzflächenforschung
14424 Potsdam, Germany *

Source:
In *Statistical Mechanics of Biocomplexity*
ed. by D. Reguera, J.M. Rubi, and J.M.B. Vilar, *Lecture Notes in Physics*,
Vol. **527**, pages 1-23 (Springer, Berlin 1999).

Abstract. On the micrometer scale, the behavior of membranes and vesicles can be understood, to a large extent, in terms of a few parameters. Two of these parameters, which are crucial for the membrane morphology, are the vesicle volume and the preferred or 'spontaneous' curvature of the membrane. † The volume is primarily determined by the osmotic conditions, i.e., by the concentration of solutes such as ions, molecules, and colloids which are dispersed in the aqueous solution and which cannot permeate the membrane. These particles can also be used to change the 'spontaneous' curvature in a systematic and controlled fashion. Another local control mechanism for this curvature is provided by molecules which are attached to the membranes via hydrophobic anchors. These control mechanisms might be used in order to construct membrane machines such as swimming vesicles which are based on cycles in shape space.

1 Introduction

Flexible membranes form the boundaries of cells and organelles and exhibit fascinating morphologies. [1] One example is shown in Fig. 1. To a large extent, this polymorphism is due to the fluidity of these membranes, i.e., to the abilitiy of the membrane molecules to move laterally within the membranes. This becomes apparent from studies of lipid bilayers and vesicles which contain only one or a few molecular components. [1, 2] Indeed, in their fluid state, these relatively simple lipid membranes already exhibit a rather complex morphology, see Fig. 2.

The polymorphism of membranes and vesicles as observed on the micrometer scale can be understood in terms of curvature models which depend only on a small number of parameters: (i) On geometric parameters such as vesicle volume and membane area and (ii) on material parameters such as 'spontaneous' curvature and bending rigidity.

*Email: lipowsky@mpikg-golm.mpg.de

†Here and below, 'spontaneous' appears in quotes since this curvature often arises from the interactions of the membrane with its surroundings.

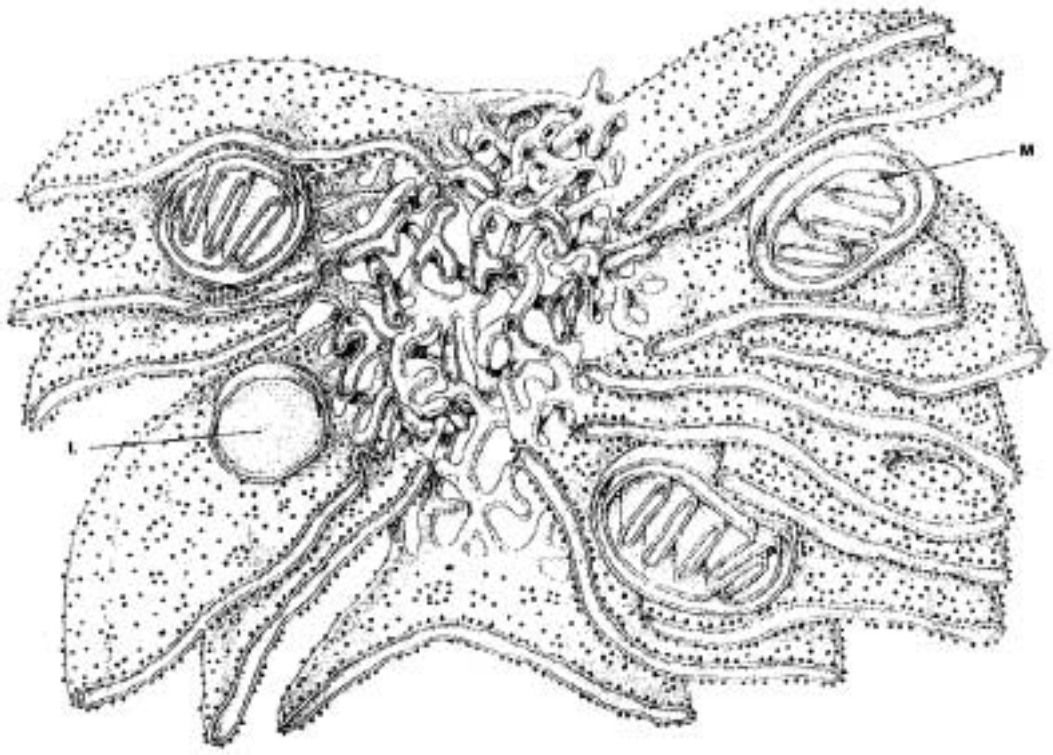

FIG. 1: Biomembranes which bound various organelles: the labyrinth of membrane sheets and tubes defines the endoplasmic reticulum; within the lamellar region, one sees the membranes of three mitochondria (M) and of one lysosom (L). (Krstic, 1976)

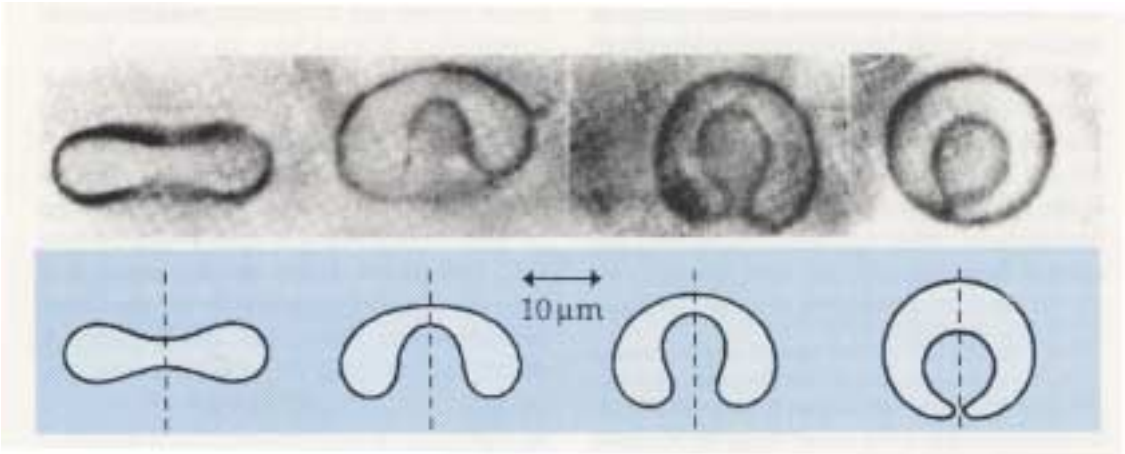

FIG. 2: Temperature–induced budding or 'endocytosis': (top) A vesicle observed by phase contrast microscopy during a temperature increase of less than one degree Celsius; (bottom) Theoretical shapes of minimal curvature energy with constraints on volume, area, and total mean curvature. The last shape on the right represents a small spherical bud which is contained in the larger sphere; both spheres are connected by a small neck or 'wormhole'.

In general, these parameters may be changed in many ways. In the present paper, I will focus on those mechanisms which are *localized* in the sense that they change the vesicle shape but leave the environment of the vesicle essentially unaffected. Two such methods are discussed in some detail: (i) particles dispersed in the interior of the vesicle; and (ii) molecules attached to the membranes by hydrophobic anchors.

The paper is organized as follows. First, I will briefly review the morphology of membranes in Section 2. The interplay of membranes with dispersed particles and anchored molecules is described in Sections 3 and 4, respectively. Finally, section 5 contains some speculations on the construction of *membrane machines* such as swimming vesicles which are based on a cyclic change of the membrane shape.

2 Membrane morphology

Single lipid bilayers form closed vesicles which can have a linear size of the order of 10 μm and which can be directly observed in the optical microscope. When the vesicle membrane is fluid, one finds a large variety of different shapes and shape transformations. One example is provided by budding processes as illustrated in Fig. 2; in this case, the vesicle develops a small interior bud and finally forms two spheres which are connected by a small neck.

The vesicle shape is governed by the curvature energies of its membrane and by constraints on the membrane area and on the vesicle volume. The area of lipid membranes is fixed (at constant temperature) because (a) the exchange of molecules between the membrane and the solution can be neglected and (b) the membrane is essentially unstretchable. Indeed, if the area of the membrane is stretched by only a few percent, the membrane ruptures. The volume of the vesicle, on the other hand, is clamped by the osmotic pressure arising from those solutes which cannot permeate the bilayer membrane, see (7) below.

The curvature energies of bilayer membranes depend on the rate at which the two monolayers exchange molecules. The basic exchange process consists of a so–called flip flop in which one amphiphilic molecule is transferred from one monolayer to the other. Two limiting cases may be considered: (i) Fast exchange and frequent flip flops on the time scales of the experiment which implies that the molecules within the membrane may easily attain their optimal packing densities in both monolayers; and (ii) Slow exchange and rare flip flops which implies that the number of molecules is kept fixed in both monolayers.

2.1 Bilayer with fast exchange between monolayers

First, consider bilayer membranes for which the molecules can easily undergo flip flops and, thus, relax local stresses induced by bending deformations. One example is provided by membranes with a large amount of cholesterol which

undergo frequent flip flops. One can then ignore the bilayer structure and treat the membrane as a surface which is characterized by its *local* geometric properties.

As one knows from differential geometry, the shape of any surface is characterized locally by its mean curvature M and its Gaußian curvature G as defined by

$$M \equiv (C_1 + C_2)/2 \qquad \text{and} \quad G \equiv C_1 C_2 \tag{1}$$

where C_1 and C_2 represent the two principal curvatures (i.e., the inverse curvature radii) at each point of the surface.

For the large vesicles considered here, the curvature radii are huge compared to the membrane thickness $l_{me} \simeq 4$ nm. One may then expand the curvature energies in powers of $l_{me} C_i$. Up to second order in the curvatures, this leads to the curvature energies [3]

$$\mathcal{E} = \oint d\mathcal{A} \;\; \{2\kappa (M - M_{sp})^2 + \kappa_G G\} \quad . \tag{2}$$

The surface integrals extend over the whole membrane surface and $d\mathcal{A}$ is the intrinsic area element. The two elastic parameters κ and κ_G have the dimensions of energy and represent the bending rigidity and the modulus of the Gaußian curvature, respectively. For closed membranes without edges, the integral over the Gaußian curvature does *not* depend on the shape of the surface but only on its topology as follows from the Gauß–Bonnet theorem.

The 'spontaneous' curvature M_{sp} in (2) describes the local asymmetry of the membrane which may arise (i) since the two monolayers of a bilayer membrane differ in their chemical composition and/or (ii) because the two sides of the membrane face different surroundings. If the membrane is symmetric, i.e., if both sides of the membrane are identical, one has $M_{sp} = 0$. In the latter case, the curvature energy as given by (2) is scale–invariant and even conformally invariant. [4]

If the bilayer membrane of a vesicle exhibits fast molecular exchange between the two monolayers, the experimentally observed shapes should correspond to those shapes which minimize the curvature energy $\mathcal{E}$ as given by (2) under the constraint of fixed surface area $\mathcal{A} \equiv 4\pi R_{ve}^2$ and fixed volume $\mathcal{V}^{in}$ of the vesicle. These minimal shapes depend only on two dimensionless parameters: (i) the reduced volume $v \equiv 3\mathcal{V}^{in}/4\pi R_{ve}^3 \leq 1$ where the equality holds for a sphere; and (ii) the reduced 'spontaneous' curvature $m_{sp} \equiv 2R_{ve} M_{sp}$. The corresponding shape diagram in the (v, m_{sp})–plane is shown in Fig. 3. [5]

2.2 Bilayer with slow exchange between monolayers

If the exchange of molecules between the two monolayers of the bilayer is sufficiently slow, each monolayer contains a fixed number of molecules. Since each of these molecules would like to occupy a certain optimal area, one obtains a constraint on the total mean curvature

$$\mathcal{M} \equiv \oint d\mathcal{A} \; M = \oint d\mathcal{A} \; \frac{1}{2}(C_1 + C_2) \tag{3}$$

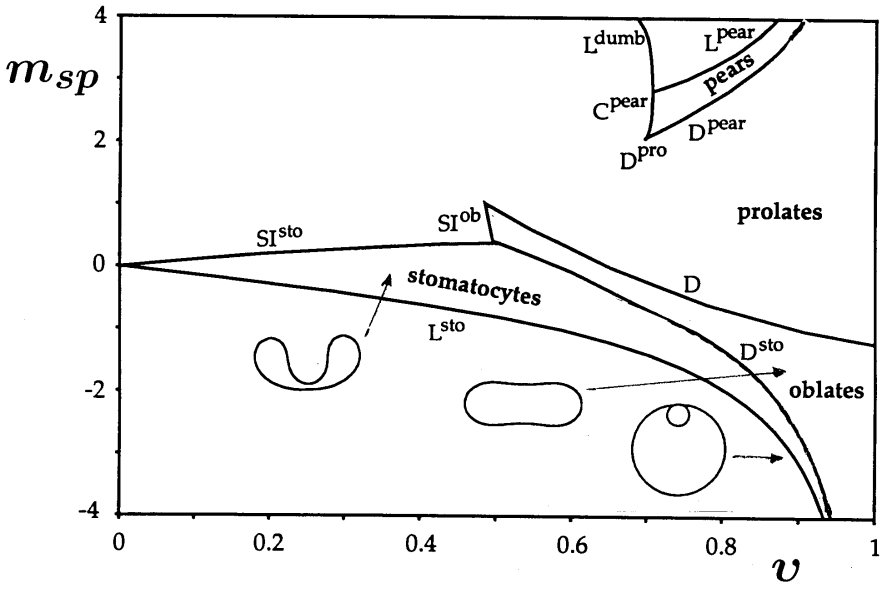

FIG. 3: Shape diagram for vesicles: *fast* molecular exchange between monolayers. The equilibrium shape is determined by the volume v and the 'spontaneous' curvature m_{sp} as defined in the text.

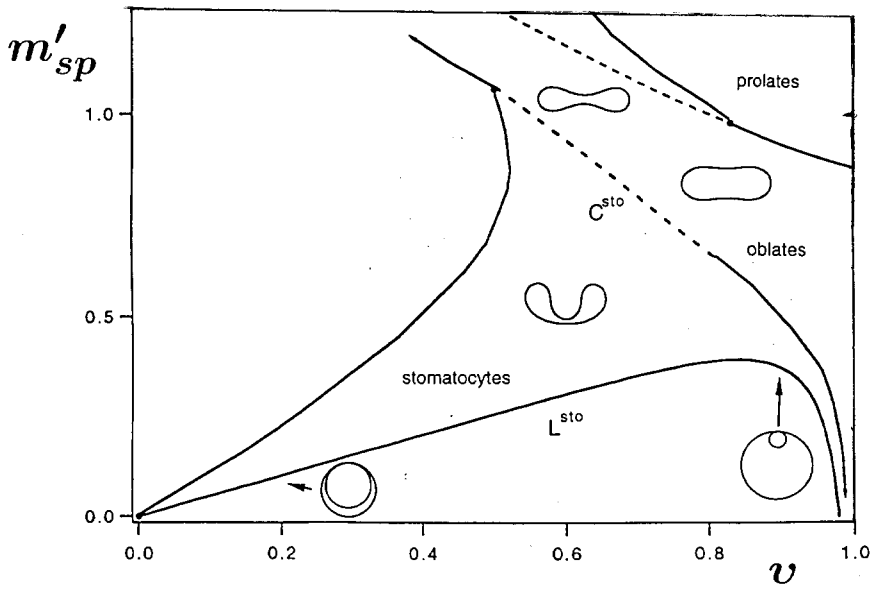

FIG. 4: Shape diagram for vesicles: *slow* molecular exchange between monolayers. (Courtesy of H. G. Döbereiner) The equilibrium shape is determined by the volume v and the effective 'spontaneous' curvature m'_{sp} as defined in the text.

which is proportional, for a *closed* bilayer membrane, to the area difference $\Delta\mathcal{A}$ of the two monolayers. In fact, $\mathcal{M}$ would like to assume the optimal value $\mathcal{M}_o$ corresponding to the optimal packing of the molecules within the monolayers. This leads to the additional curvature energy [6]

$$\bar{\mathcal{E}} = 2\pi\bar{\kappa}(\mathcal{M} - \mathcal{M}_o)^2/4\pi R_{ve}^2 \tag{4}$$

which depends on the second bending rigidity $\bar{\kappa}$ and on the vesicle radius R_{ve}. The dimensionless ratio $\bar{\kappa}/\kappa$ is expected to be of order one and $4\pi R_{ve}^2 = \mathcal{A}$ as before.

The combined curvature energy $\mathcal{E} + \bar{\mathcal{E}}$ has two terms which are linear in the total mean curvature $\mathcal{M}$. This leads to the effective 'spontaneous' curvature

$$M'_{sp} \equiv M_{sp} + \kappa\mathcal{M}_o/4\bar{\kappa}R_{ve}^2 \qquad \text{(no flip flops)} \quad . \tag{5}$$

The first term arises from $\mathcal{E}$ as given by (2) and represents the *local* 'spontaneous' curvature which depends on the local properties of the membrane and its surroundings. The second term in (5) arises from $\bar{\mathcal{E}}$ as in (4); it is a *global* quantity since it depends on the preferred value $\mathcal{M}_o$ of the total mean curvature.

Now, the vesicle shapes which are observed experimentally should correspond to those shapes which minimize the combined curvature energy $\mathcal{E} + \bar{\mathcal{E}}$ as given by (2) and (4), again under the constraint of fixed surface area $\mathcal{A}$ and fixed volume $\mathcal{V}^{in}$. These minimal shapes now depend (i) on the reduced volume v as defined previously and (ii) on the reduced 'spontaneous' curvature $m'_{sp} \equiv \kappa R_{ve} M'_{sp}/\pi\bar{\kappa}$ (normalized in such a way that $m'_{sp} = 1$ for a sphere). The corresponding shape diagram in the (v, m'_{sp})–plane is shown in Fig. 4. [7]

A more detailed discussion of curvature models and their associated shape diagrams can be found in Ref. [1] and in the review by Seifert [8].

2.3 Global versus localized control of vesicle shape

If one wants to change the vesicle shape in a systematic and controlled way, one has three possiblities: (i) Changing the membrane area; (ii) Changing the enclosed volume of the vesicle; and (iii) Changing the preferred or 'spontaneous' curvature of the membrane.

In principle, one has various control mechanisms which couple to these membrane parameters. Some of these mechanisms are *global* in the sense that they change both the vesicle and its environment. One obvious example is a change in temperature which represents the most convenient way to change the membrane area.

In the following, I will focus on *localized* control mechanisms by which one can change the vesicle shape but leaves its environment essentially unaffected. Several examples for such localized mechanisms will be discussed: (i) Control of the vesicle volume by changing the number of particles dispersed *within* the vesicle; (ii) membrane curvature induced by the interaction of such particles with the membrane; and (iii) local control of curvature by molecules anchored to the membrane.

3 Membranes and dispersed particles

The behavior of membranes in contact with dispersed ions, molecules and colloids is governed by the interplay of entropic and enthalpic forces. The entropic contribution arises from the loss of *translational* entropy of the particles in front of the membrane/solvent interfaces. This occurs as soon as the dispersed particles *cannot permeate* the membrane on the experimentally relevant time scales.

In the presence of such particles, one must first consider osmotic effects since the lipid bilayers are permeable to water molecules. As a consequence, the volumes of the two water compartments, which are separated by the membrane, will adapt until the system is osmotically balanced. In addition to these osmotic effects, the dispersed particles also affect the curvature of the membrane since they change the interfacial tensions of the two membrane/solvent interfaces. Three cases must be distinguished: [9] (i) Nonadhesive particles which are repelled from the membrane surfaces; (ii) Small adhesive particles with a size which is smaller than the membrane thickness; and (iii) Large adhesive particles with a size which is larger than the membrane thickness.

The curvature effects discussed here are accessible to experimental studies of vesicles. Recently, this approach has been used for vesicles in solutions of glucose and raffinose. [10] The values for the 'spontaneous' curvature which have been deduced in this way are in fair agreement with the theoretical results as reviewed in the following subsections.

3.1 Osmotic balance

The membrane of a closed vesicle divides space into an interior (in) and an exterior (ex) compartment with volumes $\mathcal{V}^{in} \sim R_{ve}^3$ and $\mathcal{V}^{ex}$, respectively. Both compartments may contain different particle species labeled by j. For dilute solutions, the osmotic pressure ΔP across the membrane is given by $\Delta P = T(N^{ex} - N^{in})$ with $N^{\alpha} \equiv \sum_j N_j^{\alpha}$ where N_j^{α} is the number densitiy (or concentration) of j–particles per unit volume with $\alpha = in, ex$.

This osmotic pressure difference is balanced by the bending rigidity κ of the bilayer membrane which leads to $N^{ex}\mathcal{V}^{in} = (N^{in}\mathcal{V}^{in} + c_P\kappa/T)$. In principle, this is a nonlinear equation for $\mathcal{V}^{in}$ since the dimensionless coefficient c_P depends on the shape and thus on $\mathcal{V}^{in}$. However, one usually has $N^{in}\mathcal{V}^{in} \gg \kappa/T$ which leads to

$$\sum_j \Delta N_j \equiv \sum_j (N_j^{ex} - N_j^{in}) \simeq 0 \tag{6}$$

where terms of order $\kappa/T\mathcal{V}^{in} \sim \kappa/TR_{ve}^3$ have been ignored.

The particle number densities N_j^{in} are given by $N_j^{in} \equiv \mathcal{N}_j^{in}/\mathcal{V}^{in}$ where $\mathcal{N}_j^{in}$ represents the number of j–particles inside the vesicle. It then follows from (6) that the vesicle volume $\mathcal{V}^{in}$ satisfies

$$\mathcal{V}^{in} \simeq \sum_j \mathcal{N}_j^{in} / \sum_j N_j^{ex} \qquad . \tag{7}$$

Thus, one may change the vesicle volume (i) by changes in the exterior number densities (or concentrations) N_j^{ex} which represent global control parameters and/or (ii) by changes in the interior particle numbers $\mathcal{N}_j^{in}$ which represent localized control parameters.

Thus, in order to control the vesicle volume without changing its environment, one has to change the particle numbers $\mathcal{N}_j^{in}$ inside the vesicle. This can be achieved, e.g., by polymerization, association and/or adsorption of the dispersed particles, see Fig. 5.

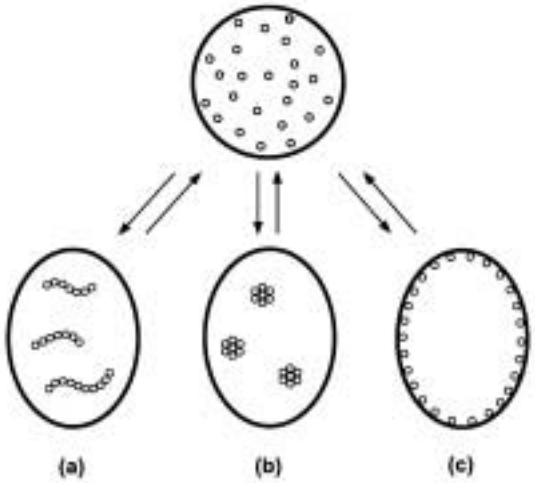

FIG. 5: Localized control of vesicle volume by (a) polymerization, (b) association, and (c) adsorption of particles dispersed inside the vesicle. The downward and the upward arrows correspond to deflation and inflation, respectively.

3.2 Non–adhesive particles

Nonadhesive particles are repelled from the membrane/solvent interfaces and thus are depleted in front of these interfaces. This depletion increases the interfacial free energy of these surfaces. [11, 12, 13] If one substracts the interfacial free energy of the flat membrane/water interfaces and balances the resulting excess free energy with the bending energy, one arrives at the 'spontaneous' curvature [9]

$$M_{sp} = -\frac{T}{4\kappa} \sum_j \Delta N_j R_j (l_{me} + R_j) \quad . \tag{8}$$

Here all particles are taken to be essentially spherical and, thus, to be characterized by a single length scale, namely their radius $R_{pa} = R_j$ for species j. In general, the bending rigidity κ may contain contributions from higher order curvature terms of the interfacial free energies.

For a closed vesicle, osmotic equilibrium implies $\sum \Delta N_j \simeq 0$ as in (6). Thus, for a solution with a single species, the 'spontaneous' curvature as given by (8) vanishes. For a binary solution with two particle species $j = 1$ and $j = 2$, one obtains $M_{sp} = (T/4\kappa)\Delta N_1(R_2 - R_1)(l_{me} + R_1 + R_2)$ which is proportional to the size difference $R_2 - R_1$. Since $\Delta N_1 = N_1^{ex} - N_1^{in}$, the membrane segment *curves toward the larger particles*, see Fig. 6 (a).

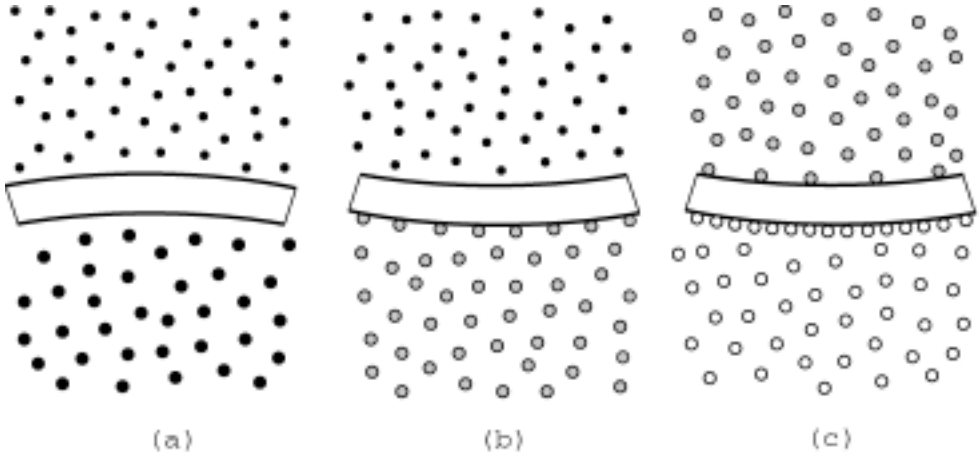

FIG. 6: 'Spontaneous' curvature of a membrane segment which is in contact with dispersed particles: (a) Two non–adhesive particle species; (b) One adhesive and one non–adhesive species; and (c) Two adhesive species.

Note that the 'spontaneous' curvature *increases* monotonically with increasing particle size. This should apply both to small particles with $R_{pa} < l_{me}$ and to large particles with $R_{pa} > l_{me}$. In both cases, the expression as given above will apply to membrane segments which are large compared to the mean distance of the dispersed particles.

3.3 Small adhesive particles

Next, consider small spherical particles with radii $R_j \ll l_{me}$ which are attracted toward the membrane surface. It follows from the Gibbs adsorption equation that the interfacial tension is reduced by adsorption. A simple estimate for this reduction can be obtained in the framework of Langmuir–type models for monolayer adsorption. [14]

If the resulting change in the free energies of the membrane/water interfaces is again balanced against the bending energy of the membrane, one now obtains the 'spontaneous' curvature [9]

$$M_{sp} = +\frac{T}{4\kappa} \sum_j k_j \Delta N_j \frac{l_{me} + 2R_{pa}}{c_{ad} R_{pa}^2}. \tag{9}$$

which increases monotonically with *decreasing* particle size (a lower cutoff is provided by the molecular roughness of the membrane surface). The Langmuir constants k_j are small and large for weak and strong j–adsorption, respectively.

A single species of adhesive particles has again no effect on the spontaneous curvature. For a binary solution with two species $j = 1$ and $j = 2$ of adhesive particles, on the other hand, the 'spontaneous' curvature as given by (9) becomes $M_{sp} = (T/4\kappa)(k_1 - k_2)\Delta N_1(l_{me} + 2R_{pa})/c_{ad}R_{pa}^2$. This implies that the membrane curves away from the more strongly adsorbed particles as in Fig. 6(c). In addition, M_{sp} *decreases* monotonically with increasing R_{pa}.

3.4 Large adhesive particles

If the particle size R_{pa} is large compared to the membrane thickness l_{me} but still small compared to the vesicle size, the competition between the adhesion energy and the bending energy now leads to a somewhat different behavior: the membrane will typically try to wrap around the particle and thus to encapsulate it.

The attractive interaction between the particle and the membrane may be described by their adhesion energy per unit area, $W < 0$. The adhesion energy is then given by $W\mathcal{A}_{co}$ where $\mathcal{A}_{co}$ is the contact area. If this adhesion energy is balanced against the bending energy of the membrane, a *single* particle is encapsulated by the membrane as soon as its size R_{pa} exceeds the threshold value [15, 9]

$$R_* \equiv [2\kappa/|W|]^{1/2} \quad . \tag{10}$$

The same threshold also applies to collapsed polymer chains which adhere to the membrane. A similar balance of adhesion and bending energies has been recently used for the case in which the attraction arises from depletion forces between small and large dispersed particles. [16] Note that the relation (10) does not include the constraints on the vesicle area and on the vesicle volume. If the particle size R_{pa} becomes of the same order as the vesicle size, these constraints act to prevent the particle encapsulation as observed in recent experiments. [17].

If the solution contains *many* adhesive particles with $R_{pa} \gg R_*$, the membrane will try to encapsulate a large number of them. If the membrane is again treated as an unstretchable surface with fixed area $\mathcal{A}$, the maximal number of particles which can be encapsulated depends on the reduced volume $v \equiv 3\mathcal{V}^{in}/4\pi R_{ve}^3 \leq 1$ of the initial state of the vesicle: The membrane can encapsulate adhering particles if its initial state has $v < 1$, i.e., as long as its initial shape is deflated compared to a sphere. The encapsulation will proceed until the membrane forms a large spherical 'mother' vesicle with many spherical buds, see Fig. 7. [9]

If some molecules such as cholesterol within the bilayer membrane can undergo relatively fast flip flops between the two monolayers, all three states displayed in Fig. 7 should be accessible. For relatively slow flip flops, on the other hand, the constraint on the area difference $\Delta\mathcal{A} \sim \mathcal{M}$ described by the curvature energy (4) favors the states shown in Fig. 7(b) for which the numbers of interior and exterior

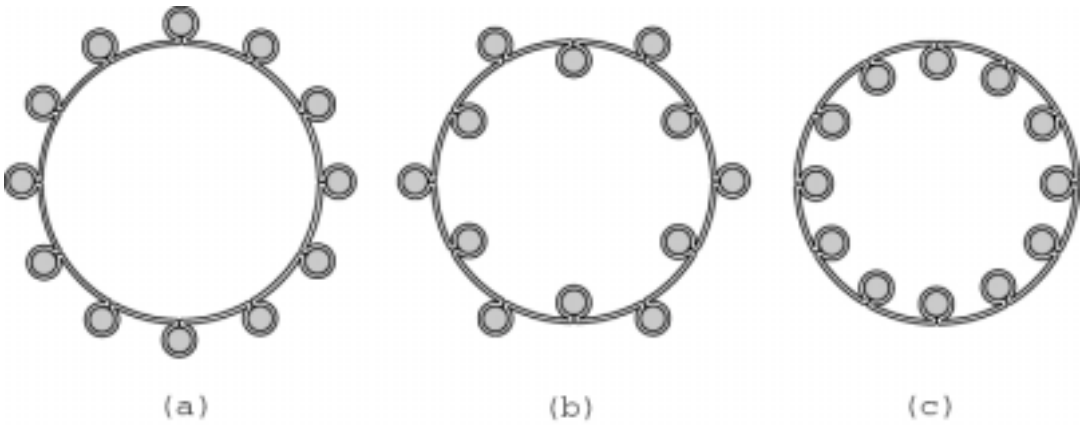

FIG. 7: Vesicle with several encapsulated particles adsorbed (a) from the interior compartment; (b) from both the interior and the exterior solution; and (c) from the exterior compartment. In order to simplify the figure, the membrane thickness and the particle size have been exaggerated compared to the vesicle size, and the thin water layers between the membrane and the particles have been omitted.

buds are comparable. The asymmetric states shown in Fig. 7(a) and (c), on the other hand, will be suppressed by this constraint since each interior bud which is not compensated by an exterior one involves a certain change in $\Delta\mathcal{A}$.

4 Membranes and anchored molecules

In this section, I will discuss the possibility to control the 'spontaneous' curvature of a fluid membrane by decorating it with anchored molecules. Two aspects will be emphasized: (i) anchored polymers; in this case, the the 'spontaneous' curvature induced by the molecules can be estimated by simple scaling laws; and (ii) anchored molecules which can undergo transitions between different conformational states and which, thus, represent switches between different 'spontaneous' curvatures in the adjacent membrane segments.

The following discussion summarizes our theoretical understanding of the curvature effects arising from anchored molecules. [18, 19, 15] Vesicles with anchored polymers have also been observed by optical microscopy [20, 21] but systematic studies of the curvature effects of these polymers are still missing.

There are various ways to attach molecules to membranes. Some possibilities for polymers are displayed in Fig. 8. I will focus on the simplest type of anchor which is provided by a lipid molecule. The anchored molecule is then bound covalently to the head group of this lipid anchor.

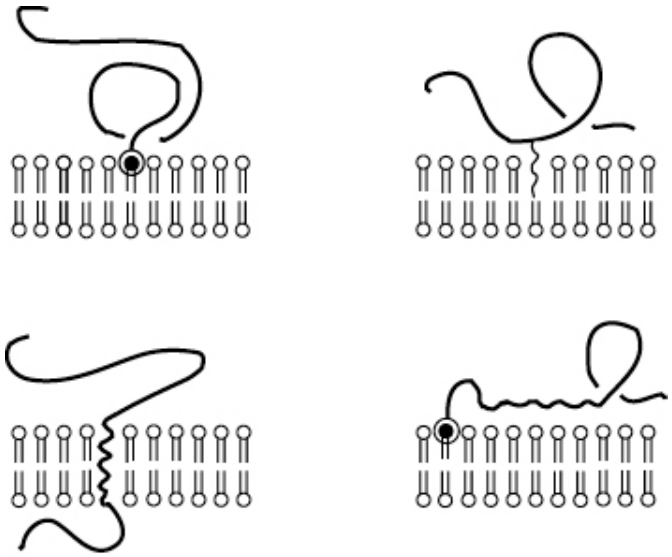

FIG. 8: Different ways to attach polymer chains to bilayer membranes: (a) Lipid anchor, (b) Hydrophobic side chain; (c) Membrane-spanning polymer segment; and (d) Anchored and adsorbed chain

4.1 Mushroom anchored at one end

First, consider a single chain for which the anchor is located at one of its ends and for which the non–anchored polymer segments experience *repulsive* interactions with the membrane surface. Such a polymer forms a *mushroom*, see Fig. 9. The size of these mushrooms is comparable to the size of the free polymer, i.e., to $R_{po} \simeq a_{po} N_{mo}^{\nu}$ with the persistence length a_{po} and the size exponent ν. The latter exponent is $\nu \simeq 3/5$ for good solvents and $\nu = 1/2$ for θ–solvents or ideal chains, see, e.g., [22].

Because the membrane reduces the configurational entropy of the mushroom, one has an entropic force which acts to bend the membrane *away* from the polymer. As a result, the adjacent membrane segment acquires the 'spontaneous' curvature [18]

$$M_{sp} \sim \ +T/\kappa R_{po} \sim \ +T/\kappa a_{po} N_{mo}^{\nu} \qquad \text{for mushrooms} \tag{11}$$

where T is the temperature in energy units.

4.1.1 Mushroom with several anchors

If the polymer chain is anchored at *both* ends, one has two competing effects. When the two ends are close together, the polymer forms an anchored ring and the membrane again bends away from the chain. On the other hand, if both ends are far apart, the polymer is in a stretched state and then pulls on the membrane. For ideal chains with $\nu = 1/2$, these two competing effects cancel to leading order. [15]

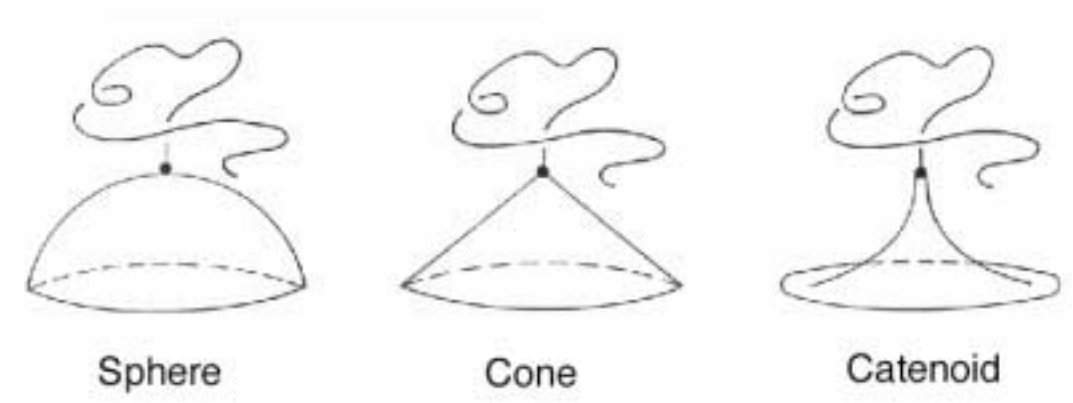

FIG. 9: Polymer mushrooms at membrane segments of different shapes which reflect the entropic repulsion between the polymer and the membrane.

Next, consider an ideal chain with several anchors which partition the chain into m segments. Its partition function factorizes into a product of m partition functions where each factor represents one chain segment. Those chain segments which are bounded by two anchors do not contribute to the 'spontaneous' curvature. Therefore, bending moments arise only from those ends which are not anchored. If both end segments are free and consist of N_1 and N_m monomers, respectively, they lead to

$$M_{sp} \simeq (T/\kappa)(R_1 + R_m)/R_{po}^2 \tag{12}$$

with $R_1 = a_{po} N_1^{1/2}$ and $R_m = a_{po} N_m^{1/2}$ for ideal chains.

4.2 Adsorbed chains

If the non–anchored segments of the chain experience *attractive* interactions with the membrane surface, the polymer will form an adsorbed *pancake*. Scaling arguments predict that the membrane now bends *towards* the polymer in order to maximize the number of contact points with the pancake. An expicit calculation for ideal chains shows, however, that the sign of M_{sp} may, in general, depend on microscopic parameters. [19]

The attractive potential between the polymer and the surface is usually described by the so–called *extrapolation length* l_{ex}, see, e.g., [23]. In general, this length scale may depend on the curvature of the surface [24] and will then behave as $l_{ex} \approx l_0(1 + l_1 M)$ for small M. For a planar surface, the inverse extrapolation length $1/l_0$ measures the distance from the adsorption transition of the ideal chain; negative and positive values of $1/l_0$ correspond to adsorbed and desorbed chains, respectively.

In the adsorbed regime (away from the adsorption transition), the 'spontaneous' curvature is found to be [19]

$$M_{sp} \simeq \lambda T/\kappa L_\perp \qquad \text{with} \quad \lambda \equiv 1 - l_1/l_0 \tag{13}$$

where $L_\perp \simeq |l_0|$ decribes the thickness of the pancake.

In principle, the relation as given by (13) predicts that the 'spontaneous' curvature induced by the pancake could have both signs depending on the relative size of the length scales l_0 and l_1. Typically, one expects to have $l_1/l_0 < 1$ which implies that the membrane bends *towards* the polymer in order to maximize the number of contact points. On the other hand, sufficiently long–ranged forces might lead to $l_1/l_0 > 1$ and, thus, to the opposite curvature. Such a non–universal behavior depending on the microscopic length scales of the system could also apply to adsorption layers consisting of many polymer chains. In the latter case, it has been proposed by de Gennes [25] that the membrane bends *away* from the adsorption layer whereas Brooks et al [26] found from a self–consistent calculation that the membrane bends *towards* the adsorbed polymers.

4.3 Anchored molecular switches

So far, I have considered anchored molecules in a certain conformation or state. Now, let us look at molecules which can attain several distinct conformations or states depending on the external conditions. In the simplest case, these molecules may assume just two different conformations, say (α) and (β).

In principle, there are many molecules which can undergo transitions between two different states. For the anchored polymers discussed in the previous subsections, two examples are (i) a polymer chains which can undergo a transition from a random coil (α) to a collapsed (or globular) state (β) ; and (ii) a polymer chain which transforms from a desorbed mushroom (α) to an adsorbed pancake (β).

In both cases, the transitions between the conformational states (α) and (β) induce changes in the 'spontaneous' curvature from $M_{sp}(\alpha)$ to $M_{sp}(\beta)$. The sign and the magnitude of these changes can be estimated using the relations (11) - (13) as given above. In particular, if the anchored polymer transforms from an adsorbed pancake to a desorbed mushroom, the preferred curvature of the adjacent membrane segment should change its sign, compare Fig. 10.

Other examples for such curvature switches are provided by molecules which can undergo transitions between a *trans* state (α) and a *cis* state (β). In general, these transitions may be triggered by various control parameters or 'effectors' such as temperature, osmotic conditions, chemical reactions and light. In some cases, the forward and the backward transition can be induced using light of two different frequencies. One interesting example is provided by azobenzene chromophores which exhibit a cis and a trans isomer, and which can be switched reversibly between these two different states using infrared and ultraviolett light, respectively.

FIG. 10: An anchored polymer which undergoes an adsorption–desorption transition induces a downward curvature $M_{sp} > 0$ for desorption (left), and an upward curvature $M_{sp} < 0$ for adsorption (right).

In summary, both dispersed particles and anchored molecules can be used in order to control the vesicle volume and the 'spontaneous' curvature of the membrane. In order to simplify the discussion in the previous sections, I have focussed on membranes which are laterally homogeneous and which are characterized by a uniform bending rigidity κ. New morphologies arise if the membranes contain distinct intramembrane domains. One example is domain–induced budding which occurs as soon as these domains are sufficiently large. [27, 28, 2]

5 Membrane machines and swimming vesicles

In this last section, I will speculate about some possibilities to construct soft matter machines which are built from membranes and vesicles. One rather obvious 'device' would be a vesicle which swims.

5.1 Basic principles of colloidal machines

In general, a colloidal machine must have three basic ingredients:
(i) A colloidal subsystem which can attain several distinct conformations or states and which is able to undergo cyclic transitions between these states;
(ii) A driving mechanism which induces such transitions and moves the subsystem out of equilibrium;
(iii) A transduction mechanism which transforms the cyclic transitions between the states into mechanical work.

In the following, I discuss shape cycles of vesicles which lead to a swimming motion. Since the vesicle size is in the micrometer range, this motion represents self–propulsion at low Reynolds number, a process which has been previously studied in some detail for bacteria and other microorganisms, see, e.g., [29].

5.2 Self–propulsion at low Reynolds number

In the limit of small Reynolds numbers, a body which swims via shape deformations has no inertia, i.e., it stops moving as soon as it stops changing its shape. This implies that the body cannot swim by 'reciprocal shape changes'. The latter type of motion corresponds to a shape sequence from S_α to S_β and back to S_α where the second sequence of shapes is the first sequence in reverse. In the absence of inertia, such a combined sequence of shape changes cannot lead to an overall center–of–mass motion of the body (this is known as the 'scallop theorem').

Thus, in order to obtain an overall motion of the center–of–mass at low Reynolds number, the body has to go through a *cycle* in shape space. It will then move by a certain distance L_{cyc} per cycle. If it takes the time t_{cyc} to perform one cycle, the swimming velocity is of the order of L_{cyc}/t_{cyc}.

5.3 Cycles in shape space

Since vesicles can attain a large variety of shapes, it is not difficult to imagine shape cycles which should lead to a swimming motion. One example is shown in Fig. 11.

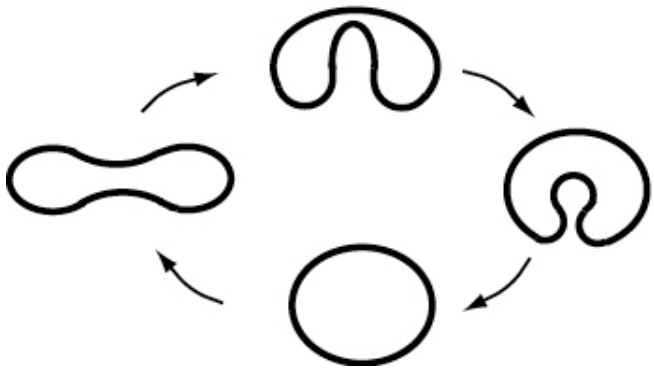

FIG. 11: Cycle in shape space which should lead to a swimming motion in the upward direction. The four steps of the cycle correspond to (I) deflation, (II) decrease of the 'spontaneous' curvature M_{sp}, (III) inflation, and (IV) increase of M_{sp}.

A shape cycle as shown in Fig. 11 corresponds to a closed path in the shape diagrams of Fig. 3 and Fig. 4. In order to perform such a cyclic change of the vesicle shape, one must, in general, change both the vesicle volume v and the membrane curvature m_{sp} (or m'_{sp}). In principle, one may also get an overall motion of the center of mass by changing only *one* parameter such as m_{sp} provided the corresponding shape trajectory moves across a discontinuous shape transfor-

mation with a hysteresis loop. However, this latter shape cycle is not expected to be very efficient.

In order to think in terms of a vesicle motor, one would like to use *localized* control mechanisms for the required shape changes. For the cycle shown in Fig. 11, the deflation and inflation steps could be obtained by using the mechanisms shown in Fig. 5, i.e., by changing the number of particles within the vesicle. The changes in the 'spontaneous' curvature, on the other hand, could be most easily done by anchored molecules which undergo transitions between distinct conformations.

As mentioned, the presumably fasted way to induce such conformational changes is by irradiation with light. One example are molecular groups which can be switched between a trans and a cis conformation by using light of two different frequencies. Likewise, one would like to use light in order to change the particle number within the vesicle. Such a control method has been realized quite recently by Petrov and Döbereiner who used the photochemical compound potassium ferrocyanide which exchanges a CN groups with a bound water molecule under illumination. [30]

5.4 Directed versus diffusive motion

The basic time scale for the shape transformation of a vesicle of linear size R_{ve} in the micrometer range is given by the relaxation time $t_{rel} \sim \eta R_{ve}^3/\kappa$ where η is the dynamical viscosity of the surrounding solution. This relation follows from dimensional analysis and was first derived for the hydrodynamic relaxation of bending modes [31].

If the control parameters can be varied sufficiently fast, i.e., on time scales which are small compared to t_{rel} (one example is provided by light), the time t_{cyc} for a cyclic shape change is set by t_{rel} and one has

$$t_{cyc} = c_o \eta R_{ve}^3/\kappa \tag{14}$$

with the dimensionless coefficient $c_o \gtrsim 1$. For lipid membranes in water, one has $\kappa \simeq 10^{-19}$ J and $\eta \simeq 10^{-3}$ Js /m^3 which leads to $t_{cyc} \simeq c_o (R_{ve}/\mu\mathrm{m})^3\, 10^{-2}$ s.

For a shape cycle as shown in Fig. 11, the translation of the vesicle arising from one such cycle will be of the order of R_{ve}. This leads to the maximal swimming velocity

$$v_{max} \simeq R_{ve}/t_{cyc} \simeq \kappa/c_o \eta R_{ve}^2 \tag{15}$$

For the aforementioned parameters as appropriate for lipid membranes in water, this leads to $v_{max} \simeq (\mu\mathrm{m}/R_{ve})^2\, (10^2/c_o)\ \mu$m/s.

The shape cycle displayed in Fig. 11 consists of shapes which are nearly axisymmetric. Thus, I tacitly assume here that this symmetry is not broken during the induced shape changes. In general, there are various ways in which this symmetry could be lost: (i) the membrane could become laterally inhomogenous or nonuniform because of domain formation or similar processes; or (ii) dynamic instabilities could lead to non–equilibrium shapes which are not axisymmetric.

If the cycle involves shapes which are far from axisymmetric, the vesicle may exhibit a tumbling motion and it is not obvious in which direction it will go. On the other hand, if the shapes in the cycle are nearly axisymmetric, the vesicle will initially move in the direction of its symmetry axis until it loses its orientation as a result of thermal fluctuations.

Indeed, as the vesicle is propelled by the shape cycle, it also undergoes translational and rotational diffusion since it is in direct contact with the surrounding solvent at temperature T. For a spherical body of linear size R_{ve}, one has the translational and rotational diffusion coefficients

$$D_{tra} = T/6\pi\eta R_{ve} \qquad \text{and} \qquad D_{rot} = T/8\pi\eta R_{ve}^3 \quad , \tag{16}$$

respectively. At room temperature $T \simeq 4\times 10^{-21}$ J, this implies $D_{tra} \simeq (\mu\mathrm{m}/R_{ve})\times 2 \times 10^{-9}$ cm^2/s and $D_{rot} \simeq (\mu\mathrm{m}/R_{ve})^3 \times 0.2$ s^{-1} for thermally–excited diffusive motion in water.

The swimming motion arising from the shape cycle will be *directed* as long as the vesicle keeps its orientation. Because of the thermal fluctuations, this orientation is lost after the rotation time

$$t_{rot} \simeq 1/D_{rot} \simeq 8\pi\eta R_{ve}^3/T \tag{17}$$

which is the time it takes to rotate the body by an angle of order $\pi/2$. This implies that the swimming motion of the vesicle exhibits the persistence length

$$\xi_{per} \simeq v_{max} t_{rot} \simeq (8\pi/c_o)(\kappa/T) R_{ve} \tag{18}$$

for a given spatial direction. For lipid bilayers in water, one has $(\kappa/T) \simeq 20$ which implies that the vesicle can be translated in a certain direction by as much as $(500/c_o)\, R_{ve}$.

For times $t \gg t_{rot}$ and length scales $L \gg \xi_{per}$, the self–propulsion of the vesicle will lead to an overall diffusive motion which is governed by the effective translational diffusion coefficient

$$D'_{tra} \simeq \xi_{per}^{\,2}/t_{rot} \simeq (8\pi/c_o^2)(\kappa^2/T\eta R_{ve}) \quad . \tag{19}$$

The usual translational motion arising from thermal fluctuations is governed by D_{tra} as given by (16). If one combines this latter relation with (19), one obtains

$$D'_{tra}/D_{tra} \simeq (48\pi^2/c_o^2)(\kappa/T)^2 \quad . \tag{20}$$

For lipid membranes with $(\kappa/T) \simeq 20$, this leads to $D'_{tra}/D_{tra} \simeq 10^4/c_o^2$. Thus, the effective diffusive motion should be much faster than the usual Brownian motion arising from thermal fluctuations.

Finally, let us check that the vesicle always stays in the low Reynolds number regime as assumed. In the present context, the Reynolds number Re is given by

$$Re = R_{ve} v_{max} \rho/\eta \simeq (1/c_o)(\kappa\rho/\eta^2 R_{ve}) \tag{21}$$

where ρ is the mass density of the solution. If one again inserts the parameters appropriate for lipid membranes and water, one obtains $Re \simeq (\mu\mathrm{m}/R_{ve})(10^{-4}/c_o)$ which is indeed quite small.

The above estimates about the swimming motion of vesicles are somewhat crude and it would be highly desirable to study this motion more systematically. From the theoretical point of view, one should then include the hydrodynamic interactions between different membrane segments as described by the appropriate Oseen tensor. This can be done with the same numerical algorithm as used previously for vesicles in an external shear flow [32].

Glossary: List of symbols

All symbols are treated as words which are ordered alphabetically.

a_{po}	persistence length of flexible polymer
$\mathcal{A}$	surface area
c	dimensionless coefficient
C_i	principal curvatures of surface with $i = 1, 2$
ΔP	osmotic pressure difference
ΔA	area difference between monolayers
$\mathcal{E}$	curvature energy of membrane
$\bar{\mathcal{E}}$	additional curvature energy for membranes without flip flops
η	dynamical viscosity
D_{tra}	diffusion coefficient for translational diffusion
D_{rot}	diffusion coefficient for rotational diffusion
G	Gaußian curvature
κ	bending rigidity
κ_G	modulus of Gaußian curvature
$\bar{\kappa}$	second bending rigidity
l_{me}	thickness of membrane
l_{ex}	extrapolation length for polymer adsorption and desorption
L	characteristic length
M	mean curvature of the membrane surface
m_{sp}	reduced, dimensionless 'spontaneous' curvature
M_{sp}	preferred or 'spontaneous' curvature
M'_{sp}	effective 'spontaneous' curvature for membranes without flip flops
$\mathcal{M}$	total mean curvature
$\mathcal{M}_o$	total mean curvature corresponding to optimal molecular packing
N_j	particle number density of species j
N_{mo}	number of monomers of a linear polymer
$\mathcal{N}_j$	number of dispersed particles of species j
R_{pa}	linear size of dispersed particles
R_{po}	linear size of anchored polymer
R_{ve}	vesicle size as defined by the surface area

Re	Reynolds number
ρ	mass density of solvent
t	time
t_{cyc}	time for one shape cycle
t_{rot}	time to rotate diffusing body
T	temperature (in energy units)
v	reduced, dimesionless volume
v_{max}	maximal swimming velocity
$\mathcal{V}$	volume
W	adhesion energy per unit area
ξ_{per}	persistence length of swimming motion

References

[1] *Structure and dynamics of membranes*, Vol. 1 of *Handbook of biological physics*, edited by R. Lipowsky and E. Sackmann (Elsevier, Amsterdam, 1995).

[2] R. Lipowsky, Current Opinion in Structural Biology **5**, 531 (1995); and in Vol. 23 of *Encyclopedia of Applied Physics*, edited by G. L. Trigg (Wiley–VCH Verlag, 1998) p. 199.

[3] W. Helfrich, Z. Naturforsch. **28c**, 693 (1973).

[4] T. Willmore, *Total curvature in Riemannian geometry* (Ellis Horwood, Chicester, 1982).

[5] U. Seifert, K. Berndl, and R. Lipowsky, Phys. Rev. A **44**, 1182 (1991).

[6] L. Miao, U. Seifert, M. Wortis, and H.-G. Döbereiner, Phys. Rev. E **49**, 5389 (1994).

[7] H.-G. Döbereiner, Ph.D. Thesis, Simon Fraser University (1995).

[8] U. Seifert, Adv. Phys. **46**, 13 (1997).

[9] R. Lipowsky and H. G. Döbereiner, Europhys. Lett. **43**, 219 (1998).

[10] H. G. Döbereiner, O. Selchow, and R. Lipowsky, Europ. Biophys. J. (in press).

[11] S. Asakura and F. Oosawa, J. Polymer Sci. **33**, 183 (1958).

[12] E. Eisenriegler, A. Hanke, and S. Dietrich, Phys. Rev. E **54**, 1134 (1996).

[13] K. Yaman, P. Pincus, and C. Marques, Phys. Rev. Lett. **78**, 4514 (1997).

[14] J. Lyklema, *Fundamentals of Interface and Colloid Science II: Solid–Liquid Interfaces* (Academic Press, London, 1995).

[15] R. Lipowsky, H. G. Döbereiner, C. Hiergeist, and V. Indrani, Physica A **249**, 536 (1998).

[16] A. Dinsmore, D. Wong, P. Nelson, and A. Yodh, Phys. Rev. Lett. **80**, 409 (1998).

[17] C. Dietrich, M. Angelova, and B. Pouligny, J. Phys. II France **7**, 1651 (1997).

[18] R. Lipowsky, Europhys. Lett. **30**, 197 (1995).

[19] C. Hiergeist, V. Indrani, and R. Lipowsky, Europhys. Lett. **36**, 491 (1996).

[20] J. Simon, M. Kühner, H. Ringsdorf, and E. Sackmann, Chem. Phys. Lipids **76**, 241 (1995).

[21] H. G. Döbereiner, A. Lehmann, W. Goedel, O. Selchow, and R. Lipowsky, Proc. MRS Meeting, Boston 1997.

[22] P.-G. de Gennes, *Scaling concepts in polymer physics* (Cornell University Press, Ithaca, 1979).

[23] E. Eisenriegler, *Polymers near surfaces* (World Scientific, Singapore, 1993).

[24] R. Ball, M. Blunt, and W. Barford, J. Phys. A: Math. Gen. **22**, 2587 (1989).

[25] P.-G. de Gennes, J. Phys. Chem. **94**, 8407 (1990).

[26] J. Brooks, C. Marques, and M. Cates, J. Physique II **1**, 673 (1991).

[27] R. Lipowsky, J. Phys. II France **2**, 1825 (1992).

[28] F. Jülicher and R. Lipowsky, Phys. Rev. E **53**, 2670 (1996).

[29] E. M. Purcell, Am. J. Phys. **45**, 3 (1977).

[30] P. G. Petrov and H. G. Döbereiner, in preparation.

[31] F. Brochard and J. Lennon, J. Physique **36**, 1035 (1975).

[32] M. Kraus, W. Wintz, U. Seifert, and R. Lipowsky, Phys. Rev. Lett. **77**, 3685 (1996).